Radiotherapy and Oncology 201 (2024) 110572

Contents lists available at ScienceDirect

Radiotherapy and Oncology

journal homepage: www.thegreenjournal.com

Original Article

Study of upright patient positioning reproducibility in image-guided proton therapy for head and neck cancers

J. Feldman [a,1], A. Pryanichnikov [b,*,1], D. Shwartz [c], Y. Hillman [a], M. Wygoda [a], P. Blumenfeld [a], M. Marash [c], A. Popovtzer [a]

[a] Sharett Institute of Oncology, Hadassah Medical Center, Hebrew University of Jerusalem, Jerusalem, Israel
[b] Division of Biomedical Physics in Radiation Oncology, German Cancer Research Center (DKFZ), Heidelberg, Germany
[c] P-Cure Ltd./Inc, Shilat, Israel

ARTICLE INFO

Keywords:
Proton therapy
Image guidance
Upright CT
Upright treatment
Seated treatment
Treatment chair

ABSTRACT

Purpose: To evaluate the patient's positioning reproducibility during upright treatment with image-guided adaptive proton therapy (IGAPT) for head and neck cancers.
Materials and methods: 10 head and neck (H&N) patients were treated with gantry-less IGAPT, which includes daily 3D computed tomography (CT) and two 2D kilovoltage radiographs before treatment and weekly 3DCT immediately after irradiation. All procedures were performed in the carbon chair on the 6 degrees of freedom robotic positioner.
Results: Prior to treatment we registered shifts in patient positioning using 3D/3D registration at the imaging isocenter: X = -0.1 ± 3.9 (mean ± standard deviation) mm, Y = −3.7 ± 3.5 mm, Z = 0.5 ± 6.2 mm. The corresponding vector was applied to the robotic positioner to compensate for the registered shifts, after which the patients were moved to the treatment isocenter and the following shifts were obtained there using 2D/3D registration: X = -0.31 ± 1.37 mm, Y = −0.02 ± 1.33 mm, Z = 0.59 ± 1.55 mm. Finally, the weekly follow-up 3D/3D registration showed X = -0.2 ± 1.2 mm, Y = −0.0 ± 1.4 mm, Z = 2.3 ± 2.0 mm.
Conclusions: A novel image-guided gantry-less PT facility showed reliable results in terms of patient positioning for H&N cases during clinical trials. This fact confirmed the suitability of using gantry-less PT for H&N treatment. A small, systematic shift in the vertical direction was detected in the follow-up 3D/3D registration. The effect of this shift will be investigated in further studies with pre/post treatment 2D/3D registration. The next phase of the clinical trial of this facility is dedicated to the thorax region.

Introduction

Image-Guided Adaptive Proton Therapy (IGAPT) is an advanced form of proton therapy (PT) used in radiation oncology to treat cancer. It combines the precision of PT with an adaptation of treatment plans based on changes in tumor size and shape [1]. Additionally, image guidance along with proper immobilization [2] minimizes the patient setup uncertainties [3]. This reduction is critical for the accurate delivery of PT, which is particularly sensitive to any additional uncertainties due to well-known properties of proton beams [4]. Despite advancements of modern PT, the widespread of this treatment modality is limited by the high initial price of the PT center, which is largely determined by the proton beam rotating system, or gantry [5]. One option to significantly reduce the cost and size of PT centers is the use of a fixed horizontal beam line with an upright patient positioning system [6,7,8,9]. Thus, recent studies show the reasonableness of using upright patient positioning systems for PT of the head and neck [10,11]. The standard practice in PT today is to use 3D computed tomography (CT) in the supine position for treatment planning [1,12]. However, there are concerns that the patient's anatomy may change significantly from the supine to upright position, especially for the thorax, abdomen and pelvic regions [13,14]. This should be considered when positioning the patient upright, and when using horizontal CT, additional anatomy recording in the treatment position should be performed [7].

In this paper, we investigated a novel IGAPT system that combines upright treatment and imaging in the same room. We used daily 3D/3D

* Corresponding author.
E-mail address: alexander.pryanichnikov@dkfz-heidelberg.de (A. Pryanichnikov).
[1] These authors contributed equally to this work and share first authorship.

https://doi.org/10.1016/j.radonc.2024.110572
Received 5 April 2024; Received in revised form 18 August 2024; Accepted 3 October 2024
Available online 10 October 2024

CT registration in the imaging isocenter, complemented by orthogonal X-ray based 2D/3D registration in the treatment isocenter. Following the work [15,16] on the reproducibility of patient positioning in upright treatment, we evaluated the results of the first 10 head and neck patients treated with a fully image-guided workflow in upright gantry-less proton therapy.

Materials and methods

Proton therapy equipment

The IGAPT facility used in this study is the P-Cure Proton Therapy Solution [17]. It is comprised of a compact proton synchrotron (the source of accelerated protons), a patient positioning system, and an imaging system, all located in the same protected room. The current configuration of all the equipment requires a total footprint of 12 m × 7 m, including racks with power supplies and control servers. The synchrotron produces protons over a water-equivalent range of 4 to 38 cm across 1900 energy levels. The fixed beam delivery with a scanning pencil beam allows a maximum field size of 28 × 30 cm^2 at the treatment isocenter located 70 cm from the accelerator nozzle. The pencil beam profile width at the isocenter varied with energy, ranging from 2.8 mm (250 MeV) to 7.7 mm (70 MeV).

The Patient Robotic Positioning and Imaging System (P-ARTIS) consists of

1) a patient positioning system (PPS) with a patient chair (Fig. 1A);
2) a vertical 4-dimensional computed tomography (4DCT) system that is used for treatment planning simulation, patient positioning verification prior to treatment and treatment adaptation if necessary.
3) an orthogonal 2D kilovoltage (kV) imaging system, used only for patient positioning verification in the treatment isocenter.

Patient upright positioning and immobilization

The P-ARTIS PPS kinematics are based on the Leoni Orion, a six-degree-of-freedom robotic system approved for proton therapy applications. The translational motion of the robot is determined by three axes: two orthogonal axes (X, Y) parallel to the floor of the room and a Z-axis orthogonal to them, as illustrated in Fig. 1B. The maximum travel distance is 4.880 m in the Y direction in the treatment coordinate system (CS), 1.184 m in the Z direction, and 2.230 m in the X direction. Robot geometry includes three articulations: base, elbow, and wrist. The elbow/base allows left and right ± 25° inflections, while the wrist offers ± 100° rotation, enabling full 360° access to the treatment volume via elbow/base inflection. The PPS has been calibrated for various loads up to 180 kg with ± 0.5 mm accuracy (95 % confidence).

The P-ARTIS operates with multiple chairs, depending on the

Fig. 1. The Patient Robotic Positioning and Imaging System (P-ARTIS): **A.** A leg-up chair for head and neck patients. **B.** Illustration of the P-ARTIS coordinate systems: the treatment Z-axis is always orthogonal to the floor, while the imaging Z-axis is parallel to the axis of the sub-vertical 4DCT slider.

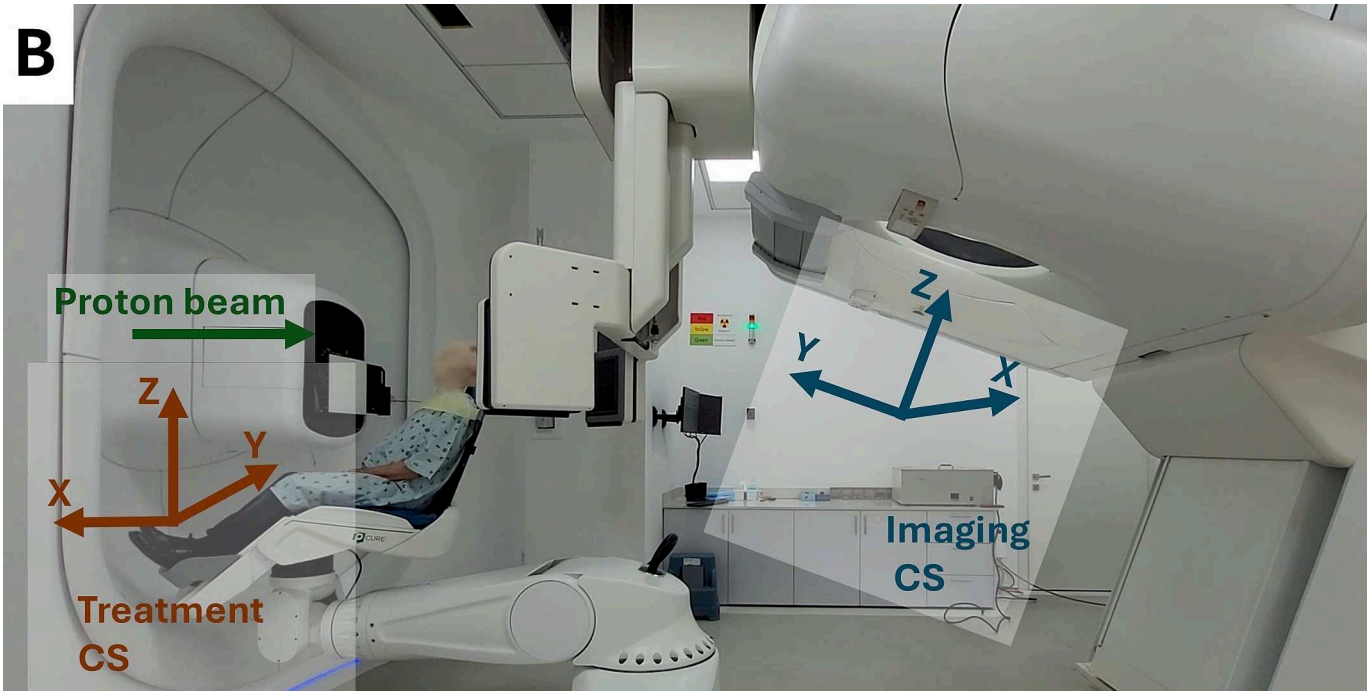

Fig. 1. (*continued*).

treatment site and patient parameters. The current study utilized the chair, as shown in Fig. 1A, in a leg-up position. This chair was used throughout the entire workflow, including initial immobilization, treatment planning simulation, daily verification procedures, and treatment. The patients were immobilized with 5-point thermoplastic masks (Orfit Ltd., Wijnegem, Belgium) fixed on the chair backrest according to the standard procedure. The masks were prepared prior to treatment and in the most cases served for the entire course. In a few cases where adaptive replanning was done during the treatment session, new masks were prepared accordingly.

Patient upright imaging and positioning verification

The P-ARTIS CT utilizes a Phillips Brilliance Big Bore platform (Phillips, Netherlands) angled at 20° relative to the vertical axis of the room. The sliding platform is utilized for image acquisition on the CT base, employing the identical control interface as the conventional moving couch. The 2D kV system provides planar, orthogonal radiographic imaging of patient geometry at the treatment isocenter position. It is designed with two 150 kV X-ray sources positioned on either side of the nozzle of the proton beam delivery system and ceiling-mounted retractable 30 cm × 30 cm flat panel detectors (FPD) PaxScan 3030DX (Varian Medical Systems, USA).

Patient position verification was performed in the proprietary software based on the elastix toolbox [18,19] by comparing 2D kV radiographs with digitally reconstructed radiographs (DRRs) based on the initial full field of view (FOV) 3DCT used for treatment planning (if no treatment adaptation is required) or the last full FOV 3DCT taken during adaptive treatment. Examples of the X-ray radiographs and corresponding DRRs with contours are shown in Fig. 2A and Fig. 2B, respectively. Since this study focused only on head and neck tumors, 4DCT protocols were not used.

Daily quality assurance for positioning verification and patient workflow

The P-ARTIS was tested daily prior to treatment. The test procedure involved obtaining both 3DCT (at the imaging isocenter) and 2D kV (at the treatment isocenter) images of the custom cubic plastic phantom with 9 inserts and comparing them to commissioned images of the same phantom. The cube was manually set to PPS instead of the patient chair. This paper includes data from April 2023 to January 2024, comprising 196 treatment shifts. The pass criterion for daily QA of the 3D/3D registration was set to 1 mm and 1 degree. Daily QA for 2D kV radiographs had a pass criterion of 0.57 mm, which is equivalent to 3 pixels of flat panel detectors. If any of the tests didn't pass, appropriate changes were made, and the procedure was repeated.

The daily patient workflow during this clinical trial [20] is as follows: A radiologic technologist (RTT) (1) places and immobilizes the patient on the carbon chair of the P-ARTIS when it is in the upload position; (2) the robotic positioner moves to the imaging isocenter and the RTT leaves the room; (3) daily 3DCT is performed and the radiation oncologist reviews the image fusions with the planning 3DCT; (4) the RTT returns and visually controls the movement of the patient to the treatment isocenter; the RTT leaves the room; (5) at the treatment isocenter positioning with X-ray kV radiographs (Fig. 2A) is performed and the patient position adjusted; this step can be repeated several times until approval is received from the radiation oncologist; (6) the patient is irradiated from one field; (7) the patient is moved to the next field, where step (5) is repeated for the number of fields required (up to 3 in the current study); finally, (8) the patient is moved back to the upload position and removed from the P-ARTIS. Additional 3DCT is obtained at the end of the week, prior to step 8, when the patient is moved from the last field of irradiation directly to the imaging isocenter of the Big Bore platform and 3DCT data are obtained. The standard workflow uses 3DCT only for interfractional monitoring and 2D kV for field-to-field verification.

There are several coordinate systems used by the P-ARTIS system, but for simplicity only two main ones are described. The treatment CS is tied to the room geometry with the Z-axis orthogonal to the floor and the Y-axis along the beam, and the imaging CS is tied to the axis of the CT bore used as the Z-axis. These two main CSs are shown in Fig. 1C. For the convenience of the reader, all data in this paper are presented in the treatment CS. The patient rotation angles with respect to the beam for each field were defined by TPS and varied 360° around the Z-axis and from 2° to 30° around the horizontal axis (pitch angle), where 0° corresponds to the vertical position of the backrest (data on all angles used

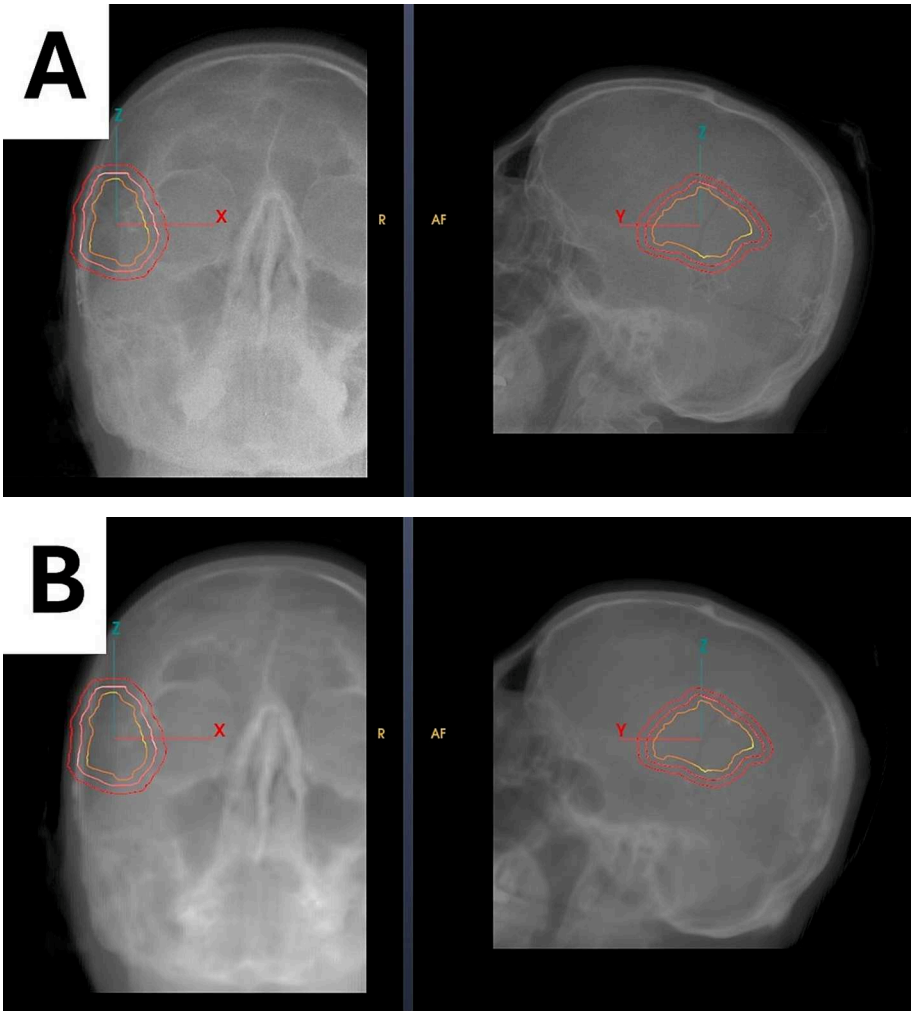

Fig. 2. The verification of patient positioning in the treatment isocenter: **A.** Example of a pair of 2D kV radiographs, **B.** Corresponding digitally reconstructed radiographs (DRRs) from the planning 3DCT.

in this study are presented in Table 4 in Appendix 1).

Patient cohorts

This study is based on the data of the first 10 patients (Table 1) treated with proton therapy at the Sharett Institute of Oncology, Hadassah Medical Center using the P-Cure PT system in Shilat in 2023. Among them, 5 patients had 35 fractions, 1 had 33, 2 had 30, 1 had 24, and 1 had 18. In total, 310 irradiation sessions were performed.

In addition, a small study (IRB study number 0048–21) was conducted in 2024 with another 4 patients to assess the patient's perception of immobilization and treatment in the upright position. Following the guidelines [14], the same questionnaire was used to assess patient comfort in different positions. The complete questionnaire can be found in Appendix 2.

Results

This paragraph is dedicated to an estimation of the rigid body positioning accuracy corresponding to the system but excluding the patient.

Table 1
Patient data.

N	Diagnosis	Height, cm	Weight, kg	N 3D/ 3D	N 2D/ 3D	N follow-up 3D/ 3D	N Fields	N Fractions
1	Buccal Mucosa	153	54.0	26	72	3	2	24
2	Buccal Mucosa	153	57.0	36	105	5	3	35
3	Maxillary sinus Carcinoma	178	78.0	33	67	6	2	33
4	Larynx Squamous Cell Carcinoma	160	57.0	36	72	5	2	35
5	Tongue Cancer	151	47.0	31	62	7	2	30
6	Salivary Gland Carcinoma	152	87.1	34	70	6	2	35
7	Nasopharyngeal Cancer	163	36.8	18	54	2	3	18
8	Oropharyngeal Squamous Cell Carcinoma with Bilateral Adenopath	186	85.6	36	69	6	2	35
9	Hypopharyngeal Cancer	162	60.9	36	108	7	3	35
10	Tongue Cancer	162.5	51.5	32	60	8	2	30

We analyzed the logged data of daily quality assurance for phantom positioning validation which included a total of 189 assessments. The 3D/3D (at the imaging isocenter) registration results were as follows: $\langle \Delta x \rangle = -0.51 \pm 0.25$ mm (mean ± standard deviation (SD)), $\langle \Delta y \rangle = 0.34 \pm 0.21$ mm, $\langle \Delta z \rangle = -0.09 \pm 0.15$ mm. All 3D/3D registered displacements are shown in the top two panels of Fig. 2 with the mean subtracted. The reason for the mean subtraction is to demonstrate the positioning reproducibility of the bare system and any systematic could be eliminated by careful calibrations. The mean positioning error was determined as a following Euclidian norm:

$$\langle \| \overrightarrow{\Delta r} - \langle \overrightarrow{\Delta r} \rangle \| \rangle = 0.31mm \quad (1)$$

For 2D/3D (at the treatment isocenter) registration, the positions of 9 inserts of the cube phantom projected onto an FPD plane were measured. Then the corresponding vectors $\overrightarrow{\Delta r_1}$ and $\overrightarrow{\Delta r_2}$ were calculated and the mean values of these 9 inserts for both FPDs were taken: $\|\overrightarrow{\Delta r_1}\| = 0.13 \pm 0.05$ mm, $\|\overrightarrow{\Delta r_2}\| = 0.09 \pm 0.03$ mm resulting in $\|\overrightarrow{\Delta r}\| = 0.16 \pm 0.05$ mm. The 2D displacement data are shown in the bottom two panels of Fig. 3.

All pre-treatment position verification QA procedures recorded a shift within the specified pass criteria (1 mm for 3D/3D and 0.57 mm for 2D/3D). Fig. 2 (right panels) showcases the results of daily positioning QA, illustrating 3D/3D and 2D/3D registration results over 10 months.

Patient positioning validation included a total of 318 daily interfraction 3D/3D (at the imaging isocenter) registrations during the study period for 10 patients and 310 irradiated fractions, as described in Table 1. The registered displacement data are presented in Table 2 in the format of mean ± SD, in the upper panel of Fig. 4 in the format of distribution of displacements, and in Fig. 5 (blue lines) sorted by patient. A corresponding vector was applied to the robotic positioner to compensate for the registered displacements, after which the patients were moved to the treatment position.

A total of 739 2D/3D (at the treatment isocenter) registrations were obtained for up to 3 irradiation fields, allowing monitoring of the intrafraction deviations per 2 to 3 beams in a treated position. The registered displacement data are shown in Table 2, the 2nd-4th panels of Fig. 4, and Fig. 5 (orange, red, and brown lines). Finally, 25 follow-up 3D/3D registrations (at the imaging isocenter) were obtained immediately after the irradiations, allowing preliminary conclusions to be drawn about intrafraction deviations compared to the time before and after treatment for some specific fractions. These registered displacement data are presented in Table 2, in the last panel of Fig. 4, and in Fig. 5 with green lines.

The results of the patient's perception regarding the comfort of different parts of the body as well as the ease of the treatment procedure are presented in Table 3.

Table 2
Registered mean ± SD shifts for all imaging modalities of patient positioning verification.

Scenario	⟨Δx⟩, mm	⟨Δy⟩, mm	⟨Δz⟩, mm	⟨Δφx⟩, deg	⟨Δ φy⟩, deg	⟨Δ φz⟩, deg
3D/3D Prior	−0.1 ± 3.9	−3.7 ± 3.5	0.5 ± 6.2	−0.6 ± 1.8	−0.3 ± 1.4	−0.3 ± 1.5
2D/3D Field 1	−0.55 ± 1.37	0.03 ± 1.28	0.51 ± 1.48	−0.08 ± 1.02	−0.03 ± 0.71	−0.07 ± 0.82
2D/3D Field 2	−0.20 ± 1.37	−0.00 ± 1.37	0.77 ± 1.69	−0.14 ± 0.86	0.01 ± 0.67	−0.04 ± 0.69
2D/3D Field 3	0.09 ± 1.24	−0.28 ± 1.35	0.27 ± 1.19	0.04 ± 0.39	0.04 ± 0.39	0.04 ± 0.39
2D/3D Mean	−0.31 ± 1.37	−0.02 ± 1.33	0.59 ± 1.55	−0.09 ± 0.89	−0.01 ± 0.66	−0.04 ± 0.72
3D/3D Follow-up	−0.2 ± 1.2	−0.0 ± 1.4	2.3 ± 2.0	−0.4 ± 0.8	0.0 ± 0.6	0.1 ± 0.7

Discussion

The idea of proton therapy facilities without classical beam delivery systems including gantry is currently being actively promoted in the proton and ion therapy community for a wider dissemination of this treatment technique [3,8,9]. With the rejection of the gantry, modern PT systems can already fit into treatment rooms originally designed for linear accelerators, but the low availability of clinical data is a major limiting factor. To further support the idea of gantry-less delivery of

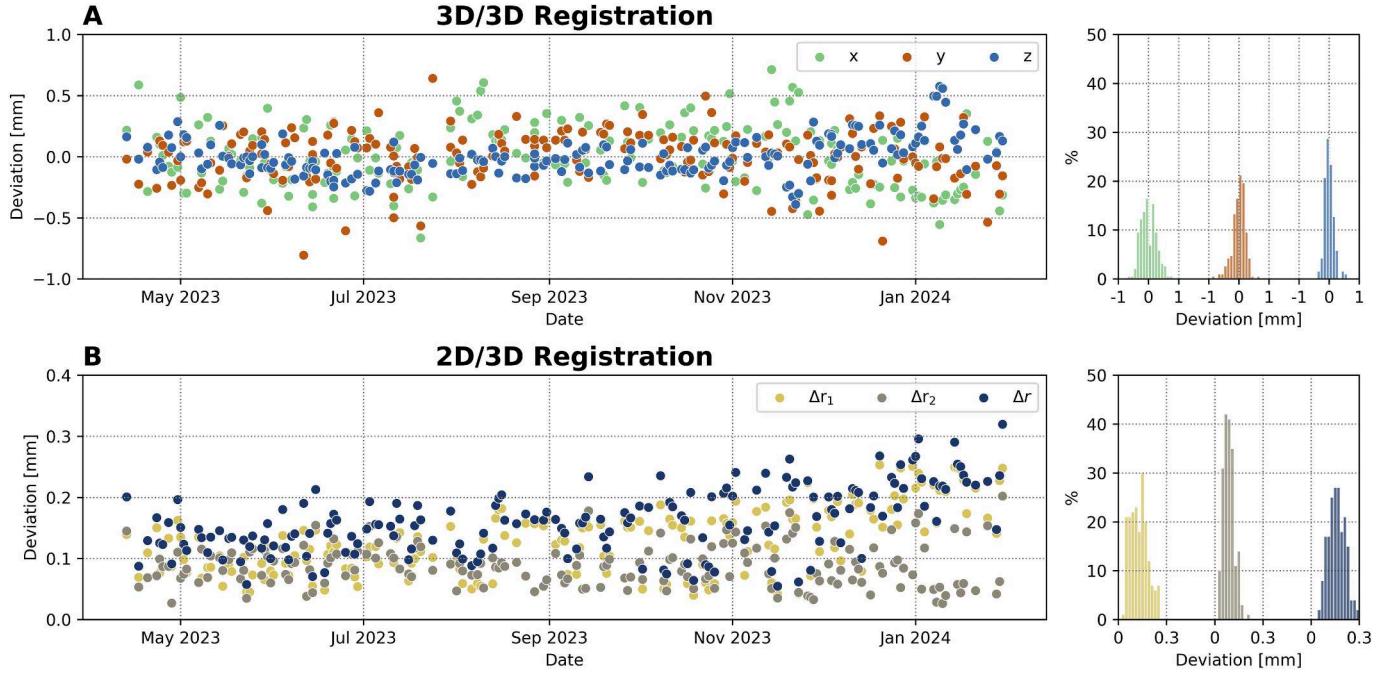

Fig. 3. Results of daily positioning QA: Panels A and B show 3D/3D and 2D/3D registration results over 10 months, and the distribution of registered 3D/3D and 2D/3D shifts, respectively. For 3D/3D registration results, the mean values were subtracted.

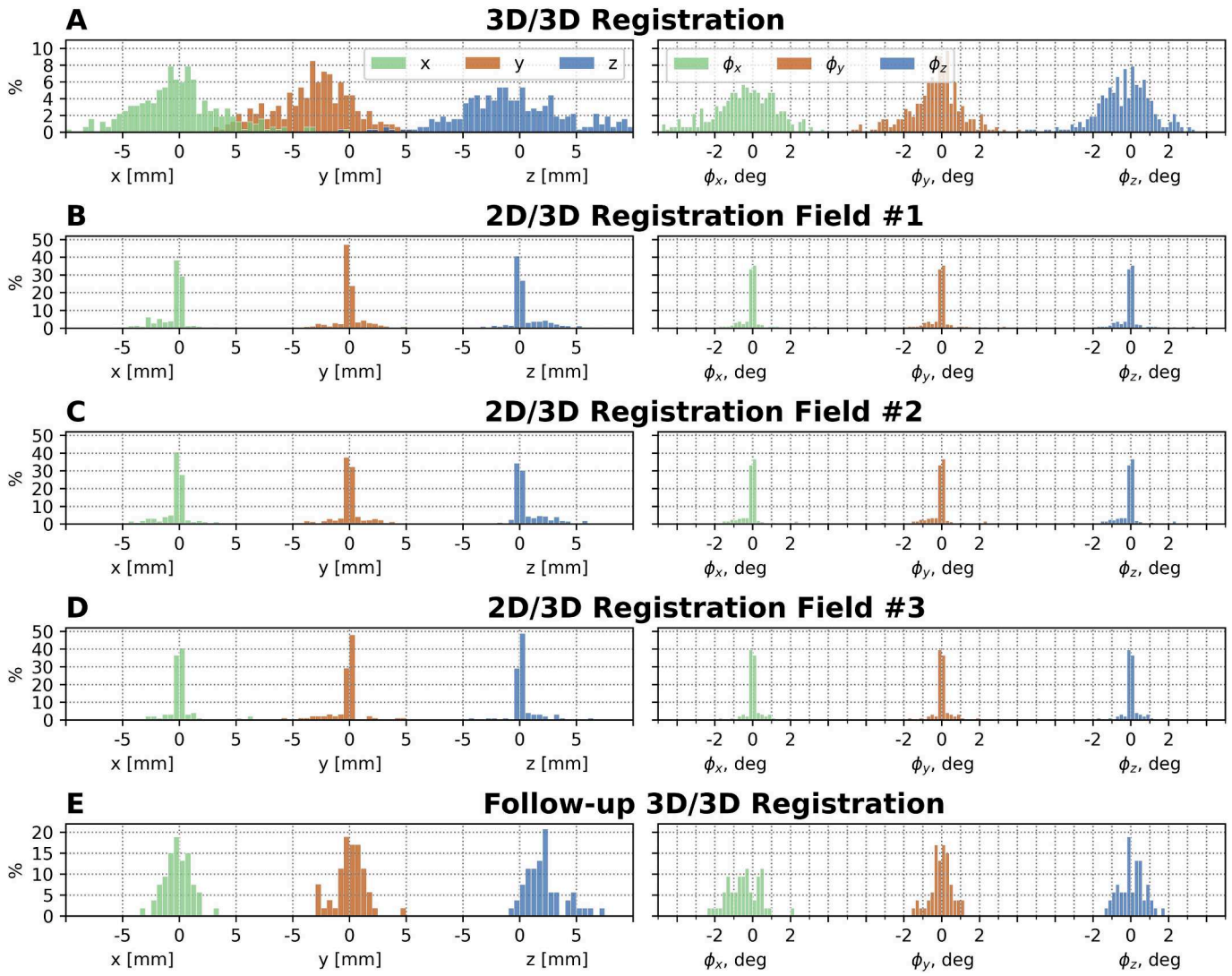

Fig. 4. Distribution of registered shifts for all imaging modalities.

proton therapy, we monitored positioning parameters during upright (in a seated position in this paper) treatments of cancer patients with malignancies in the head and neck (H&N) anatomy. Specifically, we addressed: (1) interfractional positioning accuracy daily prior to treatment, (2) intrafractional positioning accuracy per treatment field, and (3) weekly intrafractional patient position rigidity, monitored by registering the shift in patient position over the entire length of the fraction (follow-up). Although we do not continuously control the intrafractional positioning accuracy of the patient, the 2D/3D shifts and subsequent displacement can be considered as an estimate. The idea behind this is the following: recorded 2D/3D shifts are part of the routine workflow, when applied, the positioning accuracy was decided to be unacceptable. Therefore, the final positioning error is less than the applied shifts.

The accuracy of the positioning reproducibility of the system considered in this work can be benchmarked against analogous systems employing common image-guided radiation therapy (IGRT) QA protocols reliant on 2D/3D registration data. The documented mean displacements, reported at 0.16 ± 0.05 mm (with an absolute deviation of less than 0.3 mm based on the reading of one of the FPD panels), can be juxtaposed with hexapod-based systems, as detailed by Meyer et al. (translational accuracy is ranging from 0.1 mm to 0.2 mm, and rotational one between 0.10° to 0.20°) [21], and those outlined by Sheng et al. (up to 0.26 ± 0.03 mm and 0.09 ± 0.01°) [22]. Similarly, assessments conducted by Takakura et al. on 6D robotic systems (mean values 0.07 ± 0.22 mm and -0.05 ± 0.14°) [23] provide a basis for comparison. For the current study, the accuracy was always better than 1 mm for both 2D/3D and 3D/3D registration scenarios.

However, the literature on 3D/3D registration data for upright radiotherapy is scarce, likely due to the lack of vertical CT in the clinical systems described. Ongoing research efforts, as exemplified by Boisbouvier et al. [14], are attempting to fill this gap, but the timeline for clinical implementation remains indeterminate.

Mean interfraction values based on daily 3D/3D registration prior to treatments ranged from -3.7 ± 3.5 mm to 0.5 ± 6.2 mm for translational shifts and from 0.6 ± 1.8° to 0.3 ± 1.5° for rotational shifts. In particular, the reliance of the system on a fully integrated approach without laser-based initial positioning underscores the robustness of the values obtained. The mean intrafraction values based on 2D/3D registration prior to every irradiation filed ranged from -0.31 ± 1.37 mm to 0.59 ± 1.55 mm and -0.09 ± 0.89° to -0.01 ± 0.66°, representing the stereotactic level accuracy of the displacements. These values are particularly important because they directly demonstrate the feasibility of proper immobilization during treatment. Both the inter- and intrafraction accuracy parameters show a high positioning accuracy, which can be compared with similar studies for upright patient positioning, where the patients are initially immobilized in the treatment isocenter position and only 2D/3D registration is used, i.e. Sun et al. [7] reported

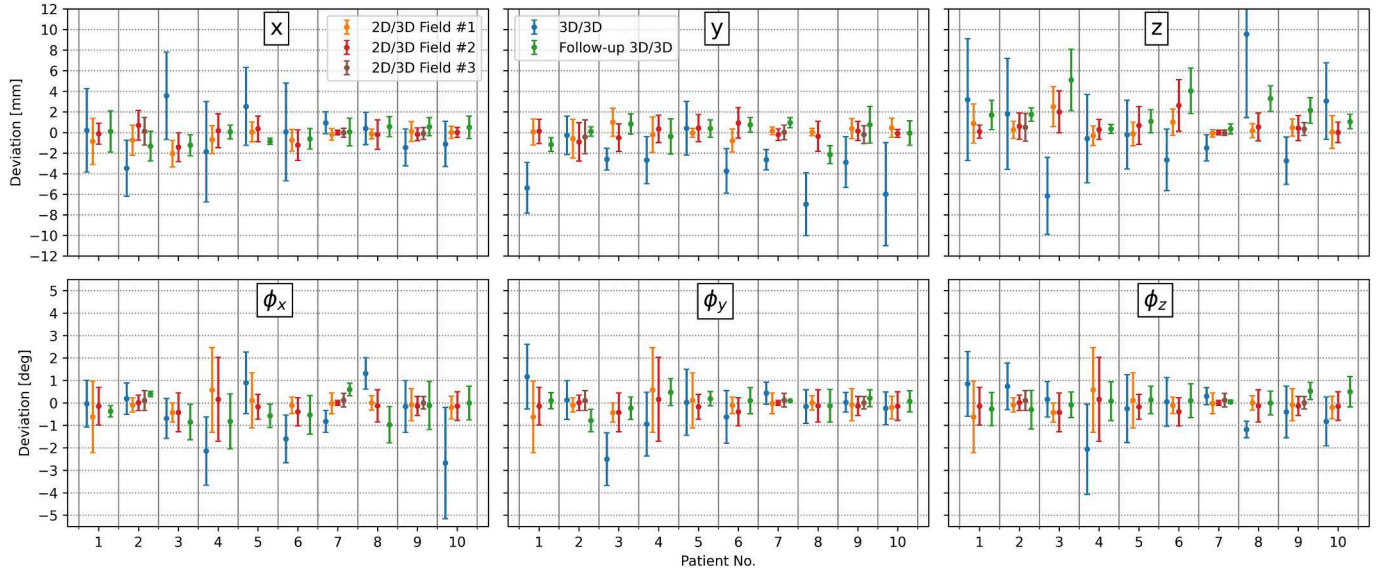

Fig. 5. Registered mean ± SD shifts for all imaging modalities sorted by patients listed in Table 1. The 3D/3D (at the imaging isocenter) represents interfraction setup variability, the 2D/3D (at the treatment isocenter) represents intrafraction uncertainty per beam, and the follow-up 3D/3D (at the imaging isocenter) represents intrafraction uncertainty for the some of the fractions.

Table 3
Patient comfort evaluation.

Scenario	Very comfortable	Comfortable	Not comfortable	Painful	Very Painful
Global comfort	1/4	1/4	2/4	0/4	0/4
Head comfort	1/4	1/4	1/4	1/4	0/4
Neck and back comfort	2/4	1/4	1/4	0/4	0/4
Arm and shoulder comfort	2/4	2/4	0/4	0/4	0/4
Abdomen comfort	2/4	2/4	0/4	0/4	0/4
Hip and leg comfort	1/4	3/4	0/4	0/4	0/4
	Very easy	Easy	Not easy but not hard	Hard	Very Hard
Easiness to setup	1/4	1/4	1/4	0/4	1/4
Easiness to get out	1/4	1/4	2/4	0/4	0/4
Easiness to breath	0/4	2/4	1/4	0/4	1/4
	Very stable	Stable	Not unstable but not stable	Unstable	Very unstable
Perception of stability	1/4	2/4	1/4	0/4	0/4

the following results for the positioning of 15 patients: 0.13 ± 0.88 mm (mean ± SD), 0.25 ± 1.17 mm, −0.57 ± 0.85 mm, 0.02 ± 0.35°, 0.00 ± 0.37°, and −0.02 ± 0.37° in x, y, z, u, v, w directions, where u, v, w − rotations. Balakin et al. [6] showed positioning results for 50H&N patients as follows: 0.1 ± 0.8 mm, −0.4 ± 2.0 mm, 0.1 ± 1.5 mm for x, y and z, respectively. McCarroll et al [15] showed results for interfractional shifts up to −1.1 ± 3.6 mm on their chair and compared these results with supine IGRT with worst mean results of 3.1 mm [24] and 1.3 ± 2.5 mm [25]. The results obtained in this study using 2D/3D registration are comparable to other upright and prone IGRT systems. This confirms the correctness of the chosen workflow with correction of the positioning before the start of treatment.

To verify overall positional rigidity, we acquired a CT dataset once a week (when possible) after treatment, just before patients were released from immobilization. During the 30 min of immobilization, the patients remained stable overall. However, analysis of the patient's position along the vertical axis revealed slight systematic downward shifts, indicating that the patient was prone to sagging by an average of up to 2.3 ± 2.0 mm (positive number corresponds to the required upward shift), as can be seen in the fifth panel of Fig. 4 (for all patients) and Fig. 5Z (for each patient individually). This finding highlights the system's ability to detect subtle changes in patient position, thereby increasing treatment accuracy and patient safety. Since these sagging movements were not recorded during the 2D/3D registration, it can be assumed that the patient changed position after the irradiation, e.g. after relaxation. To verify the applicability of this finding to patient immobilization during treatment, further analysis of patient position immediately after treatment using kV 2D/3D (at the treatment isocenter) image registration will be addressed in the future to obtain a quantitative estimate of the intrafractional motion.

Finally, the patient's perception for four patients showed the comparable results with the study that compared upright and supine positioning [14]. The overall comfort level mean value is 3.75 vs. 4.1 for other the upright and 3.9 for the supine positions shown by Boisbouvier et al [14]. However, the current survey needs a larger group of patients to be representative of the upright treatment, since it is now influenced by many patient-specific details, for example claustrophobic fears to stay inside the CT bore during 3DCT. The current patient survey protocol is now established and will continue to collect data for future patients and different treatment sites.

To explore the possibility of using upright IGAPT in other tumor locations, the next phase of this system's clinical trial is dedicated to the thoracic region.

Conclusion

Here, we demonstrated for the first time the positioning accuracy of head and neck cancer patients treated with protons beams in a seated

position for the entire workflow, including patient immobilization accuracy, daily 3D/3D positioning accuracy registration using vertical CT, positioning accuracy for each irradiation field with kilovoltage imaging, and follow-up imaging at the end of multiple fractions for the first 10 patients. The results clearly demonstrate the feasibility of such a setup and support the idea of treating patients with a compact, gantry-less proton therapy solution.

Conflict of interest statement

Alexander Pryanichnikov has a consulting agreement with P-Cure Ltd./Inc., Dmitry Shwartz is an employee of P-Cure Ltd./Inc., Michael Marash is a founder and CEO of P-Cure Ltd./Inc.

Funding statement

P-Cure Ltd./Inc. provided financial support for this study.

CRediT authorship contribution statement

J. Feldman: Writing – review & editing, Validation, Project administration, Formal analysis, Data curation, Conceptualization. **A. Pryanichnikov:** Writing – review & editing, Writing – original draft, Visualization, Validation, Project administration, Methodology, Formal analysis, Data curation, Conceptualization. **D. Shwartz:** Writing – review & editing, Methodology, Investigation, Formal analysis, Data curation, Conceptualization. **Y. Hillman:** Writing – review & editing, Validation, Data curation. **M. Wygoda:** Writing – review & editing, Supervision, Conceptualization. **P. Blumenfeld:** Writing – review & editing, Validation, Supervision, Conceptualization. **M. Marash:** Writing – review & editing, Validation, Supervision, Resources, Funding acquisition, Conceptualization. **A. Popovtzer:** Writing – review & editing, Validation, Supervision, Resources, Conceptualization.

Declaration of competing interest

The authors declare that they have no known competing financial interests or personal relationships that could have appeared to influence the work reported in this paper.

Appendix A. Supplementary material

Supplementary data to this article can be found online at https://doi.org/10.1016/j.radonc.2024.110572.

References

[1] Lane SA, Slater JM, Yang GY. Image-guided proton therapy: A comprehensive review. Cancers (Basel) 2023;15:2555. https://doi.org/10.3390/cancers15092555.
[2] van Herk M. Errors and margins in radiotherapy. Semin Radiat Oncol 2004;14:52–64. https://doi.org/10.1053/j.semradonc.2003.10.003.
[3] Beddok A, Vela A, Calugaru V, Tessonnier T, Kubes J, Dutheil P, et al. Proton therapy for head and neck squamous cell carcinomas: A review of the physical and clinical challenges. Radiother Oncol 2020;147:30–9. https://doi.org/10.1016/j.radonc.2020.03.006.
[4] Paganetti H. Range uncertainties in proton therapy and the role of Monte Carlo simulations. Phys Med Biol 2012;57:R99–117. https://doi.org/10.1088/0031-9155/57/11/R99.
[5] Yan S, Lu HM, Flanz J, Adams J, Trofimov A, Bortfeld T. Reassessment of the necessity of the proton gantry: Analysis of beam orientations from 4332 treatments at the massachusetts general hospital proton center over the past 10 years. Int J Radiat Oncol Biol Phys 2016;95:224–33. https://doi.org/10.1016/j.ijrobp.2015.09.033.
[6] Balakin VE, Belikhin MA, Pryanichnikov AA, Shemyakov AE, Strelnikova NS. Clinical application of new immobilization system in seated position for proton therapy. KnE Energy 2018;3:45–51. https://doi.org/10.18502/ken.v3i2.1790.
[7] Sun J, Kong L, Chen Z, You D, Mao J, Guan X, et al. Clinical implementation of a 6D treatment chair for fixed ion beam lines. Front Oncol 2021;11:694749. https://doi.org/10.3389/fonc.2021.694749.
[8] Devicienti S, Strigari L, D'Andrea M, Benassi M, Dimiccoli V, Portaluri M. Patient positioning in the proton radiotherapy era. J Exp Clin Cancer Res 2010;29:47. https://doi.org/10.1186/1756-9966-29-47.
[9] Volz L, Sheng Y, Durante M, Graeff C. Considerations for upright particle therapy patient positioning and associated image guidance. Front Oncol 2022;12:930850. https://doi.org/10.3389/fonc.2022.930850.
[10] Shierlaw E, Penfold M, Crain R, Santos AMC, Penfold SN. Dosimetric comparison of gantry and horizontal fixed-beam proton therapy treatment plans for base of skull chordoma. J Med Radiat Sci 2023:1–8. https://doi.org/10.1002/jmrs.742.
[11] Gordon K, Gulidov I, Smyk D, Semenov A, Golubev K, Lemaeva A, et al. Upright proton therapy for esthesioneuroblastoma: A single-institution experience. Front Oncol 2024;14:1348291. https://doi.org/10.3389/fonc.2024.1348291.
[12] Mohan R, Grosshans D. Proton therapy - Present and future. Adv Drug Deliv Rev 2017;15:26–44. https://doi.org/10.1016/j.addr.2016.11.006.
[13] Marano J, Kissick MW, Underwood TSA, Laub SJ, Lis M, Schreuder AN, et al. Relative thoracic changes from supine to upright patient position: A proton collaborative group study. J Appl Clin Med Phys 2023;24:e14129. https://doi.org/10.1002/acm2.14129.
[14] Boisbouvier S, Boucaud A, Tanguy R, Grégoire V. Upright patient positioning for pelvic radiotherapy treatments. Tech Innov Patient Support Radiat Oncol 2022;24:124–30. https://doi.org/10.1016/j.tipsro.2022.11.003.
[15] McCarroll RE, Beadle BM, Fullen D, Balter PA, Followill DS, Stingo FC, et al. Reproducibility of patient setup in the seated treatment position: A novel treatment chair design. J Appl Clin Med Phys 2017;18:223–9. https://doi.org/10.1002/acm2.12024.
[16] Moore SJ, Herst PM, Louwe RJW. Review of the patient positioning reproducibility in head-and-neck radiotherapy using Statistical Process Control. Radiother Oncol 2018;127:183–9. https://doi.org/10.1016/j.radonc.2018.01.006.
[17] Feldman J, Pryanichinikov A. White Paper P-Cure Proton Therapy Solution. https://www.p-cure.com/wp-content/uploads/2024/04/P_Cure_White_paper.pdf.
[18] Klein S, Staring M, Murphy K, Viergever MA, Pluim JPW. elastix: A toolbox for intensity based medical image registration. IEEE Trans Med Imag 2010;29:196–205. https://doi.org/10.1109/TMI.2009.2035616.
[19] Shamonin DP, Bron EE, Lelieveldt BPF, Smits M, Klein S, Staring M. Fast parallel image registration on CPU and GPU for diagnostic classification of Alzheimer's disease. Front Neuroinfor 2014;7:1–15. https://doi.org/10.3389/fninf.2013.00050.
[20] Pivotal Study of Proton Radiotherapy Treatments Using Fixed Beam Chair-Based Delivery System (PPTS) Available at: www.clinicaltrials.gov/study/NCT05549414 (Accessed Feb. 1, 2024).
[21] Meyer J, Wilbert J, Baier K, Guckenberger M, Richter A, Sauer OA, et al. Positioning accuracy of cone-beam computed tomography in combination with a hexapod robot treatment table. Int J Radiat Oncol Biol Phys 2007;67:1220–8. https://doi.org/10.1016/j.ijrobp.2006.11.010.
[22] Sheng Y, Sun J, Wang W, Stuart B, Kong L, Gao J, et al. Performance of a 6D treatment chair for patient positioning in an upright posture for fixed ion beam lines. Front Oncol 2020;10:122. https://doi.org/10.3389/fonc.2020.00122.
[23] Takakura T, Mizowaki T, Nakata M, Yano S, Fujimoto T, Miyabe Y, et al. The geometric accuracy of frameless stereotactic radiosurgery using a 6D robotic couch system. Phys Med Biol 2010;55:1–10. https://doi.org/10.1088/0031-9155/55/1/001.
[24] Kapanen M, Laaksomaa M, Tulijoki T, Peltola S, Wigren T, Hyödynmaa S, et al. Estimation of adequate setup margins and threshold for position errors requiring immediate attention in head and neck cancer radiotherapy based on 2D image guidance. Radiat Oncol 2013;8:212. https://doi.org/10.1186/1748-717X-8-212.
[25] van Kranen S, van Beek S, Rasch C, van Herk M, Sonke JJ. Setup uncertainties of anatomical sub-regions in head-and-neck cancer patients after offline CBCT guidance. Int J Radiat Oncol Biol Phys 2009;73:1566–73. https://doi.org/10.1016/j.ijrobp.2008.11.035.